Environ. Sci. Technol. **1999**, *33,* 243−249

Photocatalytic Degradation of the Blue Green Algal Toxin Microcystin-LR in a Natural Organic-Aqueous Matrix

ANDREW J. FEITZ,[†] T. DAVID WAITE,*[,†] GARY J. JONES,[‡] BRACE H. BOYDEN,[§] AND PHILIP T. ORR[⊥]

School of Civil and Environmental Engineering, University of New South Wales, Sydney, New South Wales 2052, Australia, CSIRO Land and Water, 120 Meiers Road, Indooroopilly, Queensland 4068, Australia, Sinclair Knight Merz, 100 Christie Street, St. Leornards, New South Wales 2065, Australia, and CSIRO Land and Water, Locked Bag No. 3, Griffith, New South Wales 2680, Australia

The worldwide appearance of toxic cyanobacterial blooms in drinking water supplies has raised concerns about systemic effects on human health. Conventional water treatment methods are poor at removing low concentrations of cyanotoxins, and specialized treatment is usually necessary for treatment of contaminated water. In this study, the applicability of heterogeneous photocatalytic degradation of low concentrations of the cyantoxin microcystin-LR in a natural organic-aqueous matrix is examined using titanium dioxide as the photocatalyst. The initial rate of toxin degradation is strongly pH dependent in a manner mirrored by the pH dependence of toxin adsorption to TiO_2. Rapid degradation of toxin occurs in the acidic pH range in the presence of light and TiO_2 with a maximum initial rate of degradation occurring at pH 3.5, while at higher pH, a distinct lag is observed prior to commencement of toxin degradation. It is proposed that in the pH range where microcystin-LR adsorbs to TiO_2, it is degraded principally by long-lived organic radicals generated through oxidation of adsorbed cyanobacterial exudate. At higher pH, where microcystin-LR adsorption to TiO_2 is insignificant, it is proposed that these organic radicals diffuse into solution and (after a lag) initiate oxidation of the toxin in dissolved phase.

Introduction

Toxic cyanobacterial blooms are a common yet devastating occurrence in the inland waterways of many countries. These blooms produce a toxin that is, increasingly, causing concerns in both rural and urban environments (*1*). Increasing numbers of toxic blooms are being recorded in drinking water supplies (*2*, *3*), and there are concerns about the possible long-term effects of systemic exposure to a certain class of these toxins, the hepatotoxins, and possible links to human liver cancer (*4*, *5*). The cyanotoxin isolated for this study is an extract from a *Microcystis aeruginosa* bloom which possessed naturally high levels of the hepatotoxin microcystin-LR (abbreviated MLR below). This toxin (the structure of which is shown in Figure 1) is frequently identified in cyanobacterial blooms and is one of the most acutely toxic cyanobacterial toxins with an LD_{50} commonly reported within the 30−100 μg/kg range (i.p. mouse) (*6*, *7*). This toxin has also been shown to possess potent liver tumor-promoting activity in rats through inhibition of protein phosphatase activity (*8*).

Presently, the most common method to control cyanobacterial blooms is by dosing with copper based algicides. While this invariably destroys the blue-green cells, it is no longer considered an effective treatment method as it promotes blue-green tolerant species, destroys zooplankton, and releases toxins upon cell lysis (*9*, *10*). Traditional water treatment methods of chemical coagulation, flocculation, and sand filtration are often completely ineffective at removing cyanobacterial toxins (*11*, *12*). Treatment using chlorination requires high doses and long contact times, and there is the possibility of generating toxic byproducts such as trihalomethanes (*13*). Both powdered and granular activated carbon have proven effective but are expensive (*14*, *15*), and biological methods typically require a reaction time of hours to days (*16*, *17*) and are thus not viable. Preliminary ozonation experiments, however, have been successful in destroying microcystin-LR from both raw and clarified water (*13*, *18*) via ozonolysis of the diene system in the adda unit of the cyclic peptide microcystin-LR yielding inactive byproducts (*19*, *20*).

Photocatalytic oxidation is a highly effective means for water decontamination with mineralization of toxic organics to carbon dioxide, water, and mineral acids in many instances (*21*). Near ultraviolet (UV) light impinging on TiO_2 surfaces generates electron hole pairs which, unless they recombine, may result in the production of hydroxyl radicals ($OH^{\bullet}$) from either oxidation of H_2O/OH^- at photogenerated holes or via an oxygen reduction pathway (*22*, *23*). These extremely reactive hydroxyl radicals are considered to be the primary means of organic degradation (*24*). Electron acceptors other than O_2, such as IO_4^-, BrO_3^-, ClO_3^-, ClO_2^-, and H_2O_2, have also shown similar, if not greater, rates of degradation (*25*, *26*). Titanium dioxide, particularly the anatase crystalline form, is often used as a photocatalyst since it has strong oxidizing properties, is relatively inexpensive and nontoxic, and is photoactive with UV/near-UV irradiation up to a wavelength of around 380 nm (thus encompassing a small percentage of the solar spectrum). Photocatalytic oxidation is not limited to the use of TiO_2; metal semiconductors such as ZnO, CdS, WO_3, and SnO_2 have also been used for the degradation of environmental contaminants (*27*, *28*), and a variety of metal doped semiconductors (e.g. Pt, Pd, Ag, or Au on TiO_2) have exhibited various degrees of effectiveness (*29*, *30*).

Recent work by Roberston et al. (*31*) has shown that purified microcystin-LR is highly suspectible to photocatalytic oxidation using TiO_2 as a catalytst. In this study we examine the applicability of TiO_2 catalyzed photooxidation to trace levels of the cyanotoxin microcystin-LR (MLR) in a natural organic-aqueous matrix.

Materials and Methods

UV Lamp and Dark Adsorption Experiments. Near-UV lamp experiments were performed in a dark room with a

* Corresponding author phone: +61-2-9385 5060; fax: +61-2-9385 6139; e-mail: d.waite@unsw.edu.au.
[†] University of New South Wales.
[‡] CSIRO Land and Water (Indooroopilly).
[§] Sinclair Knight Merz.
[⊥] CSIRO Land and Water (Griffith).

10.1021/es970952d CCC: $18.00
Published on Web 12/04/1998

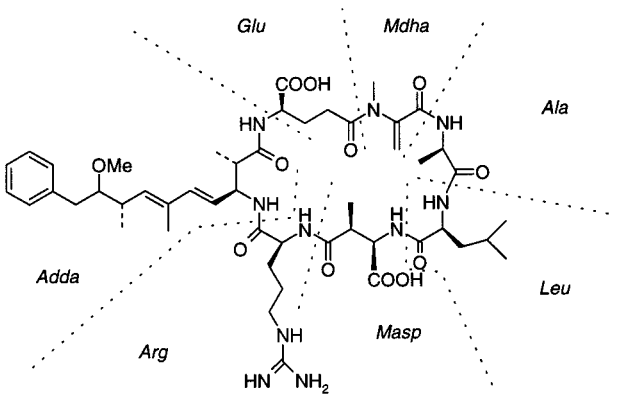

FIGURE 1. Structure of the blue-green algal toxin microcystin-LR. Besides the two variable L-amino acids, leucine and arginine, the microcystin contain three D-amino acids (glutamic acid, alanine, and methylaspartic acid) and two unusual amino acids, *N*-methyl-dehydroalanine (Mdha) and 3-amino-9-methoxy-2,6,8-trimethyl-10-phenyldeca-4,6-dienoic acid (Adda) (reproduced from ref 8).

water-jacketed borosilicate glass vessel incorporating a quartz window for illumination. Near-UV light was supplied by a 100 W high-pressure Hg arc lamp (Rofin Model No. 7730) and power supply system (Rofin Model No. 7731) with a 365 nm band pass filter (Corning No. 5970). Neutral density filters (Omega Optical Inc.) were used to adjust the irradiation intensity. Total reaction volume for each run was 140 mL with the reaction vessel continuously mixed using a magnetic stirrer. Total irradiation was determined by ferrioxalate actinometry and found to be 1600 μmol/m^2•s (i.e., approximately 52 mW/cm^2) (*32*). Spectroradiametry confirmed this result yielding 55 mW/cm^2. The titanium dioxide suspension consisted of Milli-Q (Millipore Corp.) water and Tioxide Australia TiO_2 (determined from X-ray diffraction to be principally anatase) with an average crystal size of approximately 100 nm (measured by electron microscopy). The temperature of the reaction vessel was kept constant (unless otherwise indicated) at 20.0 °C using a recirculating refrigerated water bath (Thermoline Model TBC), and pH was adjusted with 10−100 μL of 5% HNO_3 or 0.1 M NaOH depending on the required pH before injection of the microcystin-LR. At pH > 4.5, unbuffered suspensions (pH 5.0, 6.4, and 11.5) over the course of the experiment showed a decrease in pH no more that 0.5 pH units due to CO_2 dissolution, and all detailed reaction rate and adsorption studies at pH 8.6 were buffered with $NaHCO_3$. One hour dark adsorption experiments were conducted in the same reaction vessel and under similar conditions to the photodegradation studies except that the total volume of the suspension mixture in the water-jacketed Pyrex vessel was 20 mL per run. The TiO_2 concentration remained at 1 g/L to facilitate direct comparison with the photodegradation runs.

Microcystin-LR Extraction. Dried cyanobacteria, taken from a *Microcystis aeruginosa* bloom possessing naturally high levels of microcystin-LR, was suspended in Milli-Q water in two centrifuge tubes packed with ice and sonicated with a Microson Ultrasonic cell disrupter six times for 30 s. After cell disruption, the two solutions were centrifuged at 10 000 rpm for 15 min and the supernatant removed and refrigerated. The above procedure was repeated after resuspending the pellets remaining in the centrifuge tubes with additional Milli-Q water and the second supernatant added to the previous extraction mixture. The resulting blue extract was filtered through 0.2 μm cellulose acetate syringe filters and stored at −20 °C. By calibrating with a microcystin-LR standard (Calbiochem) the extract was found to contain 73 μg/mL microcystin-LR by HPLC analysis. The dissolved organic carbon (DOC) content of the sample was 2200 mg/L indicating an approximate concentration of 3 wt % MLR. The organic matter present in addition to microcystin-LR was presumably a complex mixture of cyanobacterial exudates.

The crude extract was used in all experiments rather than pure microcystin-LR because of (a) the very high cost of pure microcystin-LR, and (b) this is the mixture that would be released from a naturally lysing population of cyanobacteria. Previous studies (*33*) have shown that other cyanobacterial exudates enhance the rate of microcystin photooxidation, but as will be shown, these rates are trivial compared with the rate of TiO_2 catalyzed photooxidation.

Solar Experiments. Photocatalytic degradation studies using natural solar radiation were undertaken in a small beaker filled with a 20 mL suspension containing 1 g/L of TiO_2 and 560 μg/L of microcystin-LR crude extract in Milli-Q water. This was placed outside on a clear sunny day at noon clear of any obstructions. The temperature of the sample was measured and found to reach approximately 25 °C. The average solar irradiation in the near UV range (300−400 nm) for a clear spring and clear summer's day from global irradiance data is approximately 3.9 and 4.4 mW/cm^2, respectively (*34*). As a comparison with UV lamp experiments in the absence of TiO_2, the effect of solar radiation alone was examined under identical conditions (i.e. in a 140 mL solution in which the initial microcystin-LR concentration was 85 μg/L).

HPLC Analysis, DOC, and Sampling. High Performance Liquid Chromatography (HPLC) analysis was conducted with Waters 6000A and M-45 pumps, a Waters 660 solvent programmer, and an Alltech Spherisorb ODS-2 column (5 μm, 250 mm × 4.8 mm). The mobile phase consisted of a 5 min linear gradient of 20−35% acetonitrile in 7 mM ammonium acetate aqueous buffer solution. A Spectra-Physics rapid scanning detector acquired UV spectra (200−300 nm) at 5 nm intervals, and concentrations were determined by comparing peak area (or peak heights for concentrations less than 50 μg/L) at 240 nm with that of the standard microcystin-LR (Calbiochem). The minimum detectable amount of microcystin-LR on the column without concentration steps were 1 and 0.2 ng, quantitatively and qualitatively, respectively. This corresponds to microcystin-LR concentrations of 5 and 1 μg/L. Determination of the extent of cyanobacterial exudate adsorption on TiO_2 was measured via DOC measurements using either a Skalar instrument incorporating a persulfate/UV digestion system or a Shimadzu 5000A combustion system. Sampling for experiments consisted of withdrawing 1 mL aliquots using a micropipet, centrifuging samples in a microcentrifuge for 10 min at 13 000 rpm, and holding at 4 °C before analysis. If after centrifugation the sample was still cloudy (particularly at low pH) the samples were filtered through a 0.2 μm cellulose acetate syringe filter. For dark experiments all samples were filtered through MilliQ flushed 0.2 μm cellulose acetate syringe filters.

Results

The concentrations of MLR remaining in pH 6.4 solutions over time in the absence and presence of TiO_2 and in the absence and presence of light are shown in Figure 2. It is clear that essentially no degradation occurs in the absence of either the catalyst or light, while an initial rate of degradation of MLR of 6×10^{-11} M/s is observed in the presence of both catalyst and light and, under such conditions, the concentration of MLR is reduced from 85 to 1 nM in approximately 30 min. These results support the hypothesis that a TiO_2 catalyzed photodegradation process accounts for the reduction in concentration of microcystin-LR and suggests that homogeneous photodegradation of MLR (as previously noted by Tsuji et al. (*33*)) is not a significant process under these conditions. The effects of pH, however,

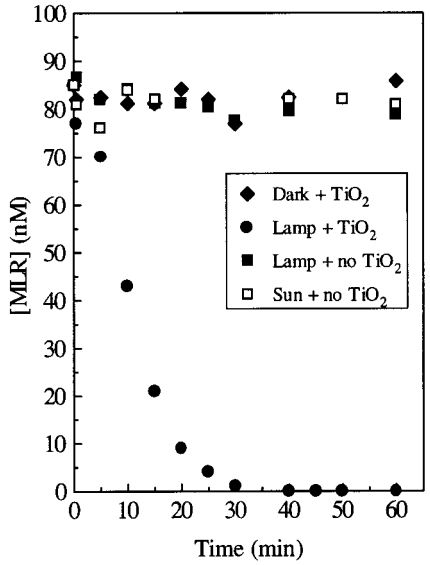

FIGURE 2. Loss of microcystin-LR from solution at pH 6.4 over time in the presence and absence of added TiO_2 and in the dark and light (both near-UV lamp photolysis and solar radiation). All runs at initial toxin concentration of 85 nM and TiO_2 loading of 1 g·L^{-1} except for Lamp with TiO_2 run where [TiO_2] = 0.5 g·L^{-1} (optimized catalyst concentration).

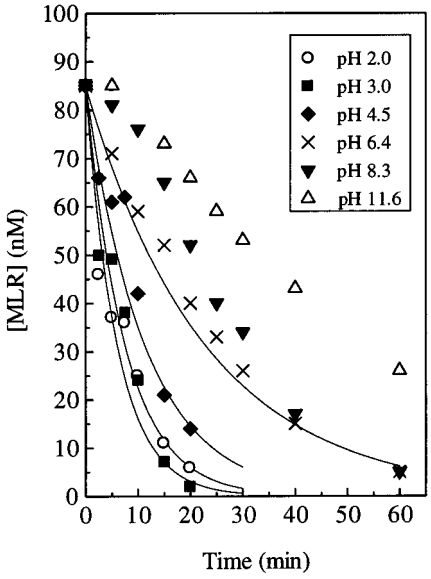

FIGURE 3. Loss of microcystin-LR from solutions of various pH. All runs at initial toxin concentration of 85 nM and TiO_2 loading of 1 g·L^{-1}. Solid lines represent exponential functions of best fit to data for pH 2.0−6.4.

as demonstrated later in this study, are a dominant factor. Log transformation of the TiO_2-catalyzed photodegradation of MLR suggests that pseudo-first-order kinetics are followed under these conditions with a pseudo-first-order rate constant (k') of 0.044 min^{-1}.

As can be seen from Figure 3, the rate of degradation increases with decreasing pH down to a pH of around 3 below which the toxin appears to be slightly more stable. An exponential decrease in MLR concentration with time is observed under acidic pH conditions. Under alkaline conditions, significantly slower initial rates of MLR decay are observed than under acidic conditions. In these high pH cases, an initial lag in degradation is observed with a subsequent increase in rate of MLR decay.

The dramatic effects of pH are clearly shown in Figure 4 where initial rates of photodegradation are plotted as a

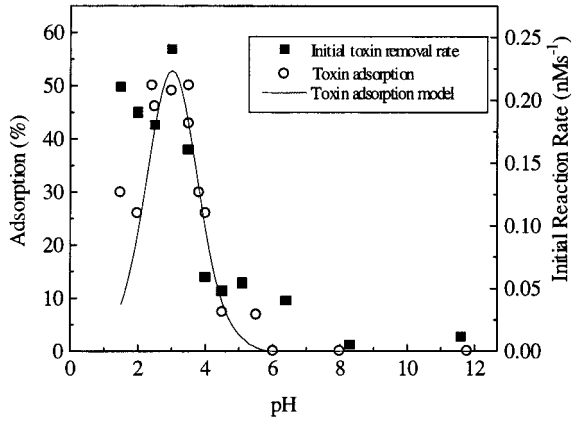

FIGURE 4. Percentage of 85 nM microcystin-LR removed at various pH after 1 h contact time with 1 g·L^{-1} TiO_2 in the dark. The solid line represents the percentage of 85 nM MLR adsorption to 1 g·L^{-1} TiO_2 as a function of pH predicted using a surface complexation model (see text). The initial removal rate of microcystin-LR from solution in the light is also shown as a function of pH.

function of suspension pH. Significantly, the pH dependence of the initial MLR photodegradation rate is approximately mirrored by the extent of MLR adsorption to TiO_2 as a function of pH. Under alkaline conditions, where toxin adsorption to TiO_2 appears to be minimal, the initial degradation rates are essentially zero though, as noted above, significant degradation is observed at later times (Figure 3).

While the pH dependencies of MLR adsorption and initial toxin photodegradation rates mirror each other closely, the dependencies of extent of toxin adsorption and photodegradation behavior on added toxin concentration appear to be rather dissimilar. As shown in Figure 5a, increasing uptake on increasing MLR concentration is initially observed but with saturation of extent of adsorption at higher toxin concentrations. This adsorption data is adequately described by a Langmuir isotherm expression; i.e.,

$$[\mathrm{MLR}]_{ads} = \frac{K_{ads}\cdot[\mathrm{MLR}]_{ads}^{max}\cdot[\mathrm{MLR}]_{soln}}{(1 + K_{ads}\cdot[\mathrm{MLR}]_{soln})} \quad (1)$$

where $[\mathrm{MLR}]_{soln}$ and $[\mathrm{MLR}]_{ads}$ are the concentrations of toxin in solution and on the solid respectively after 1 h contact with the solid, K_{ads} is the conditional equilibrium constant (for formation of an adsorbed toxin species), and $[\mathrm{MLR}]_{ads}^{max}$ represents the maximum concentration of toxin that may be adsorbed to the TiO_2 surface (within the 1 h equilibration time allowed). Linear transformation of eq 1 yields an expression of the form

$$\frac{[\mathrm{MLR}]_{soln}}{[\mathrm{MLR}]_{ads}} = \frac{1}{[\mathrm{MLR}]_{ads}^{max}}[\mathrm{MLR}]_{soln} + \frac{1}{K_{ads}\cdot[\mathrm{MLR}]_{ads}^{max}} \quad (2)$$

which, when fitted to the available data (Figure 5b), provides an estimate for K_{ads} of $10^{6.8}$ M^{-1} and for $[\mathrm{MLR}]_{ads}^{max}$ of 128 nM (at pH 3.5). Given that 1 g/L of TiO_2 has been used in these adsorption studies, this represents a maximum adsorption density of 128 nmol of toxin per gram of TiO_2 at pH 3.5. Using data from Roberston et al. (*31*) who used micromolar concentrations of purified MLR (i.e. 1000-fold higher than used in this study) at pH 4.0 on Degussa P-25 TiO_2, a K_{ads} of $10^{4.1}$ M^{-1} may be determined.

In comparison with the Langmuirian behavior of MLR adsorption, the rate of MLR loss from solution is observed to decrease on increasing the concentration of added toxin (and, concomitantly, other cyanobacterial exudate) (see Figure 6). At low pH and low MLR concentrations, degradation is pseudo-first-order (as is also apparent from Figure 3)

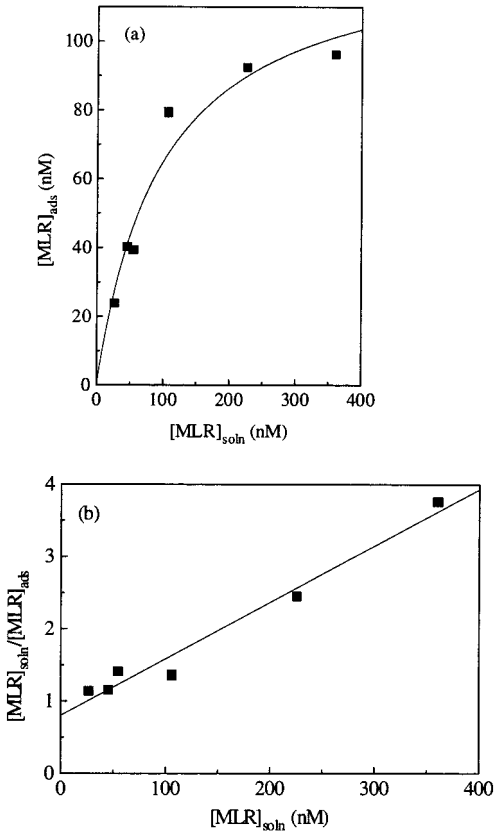

FIGURE 5. Concentration of MLR adsorbed to 1 g·L^{-1} TiO_2 at pH 3.5 as a function of the solution concentration of the toxin (Figure 5a). The solid line through the data represents the rectangular hyperbola of best fit as determined by linear transformation of the data (Figure 5b).

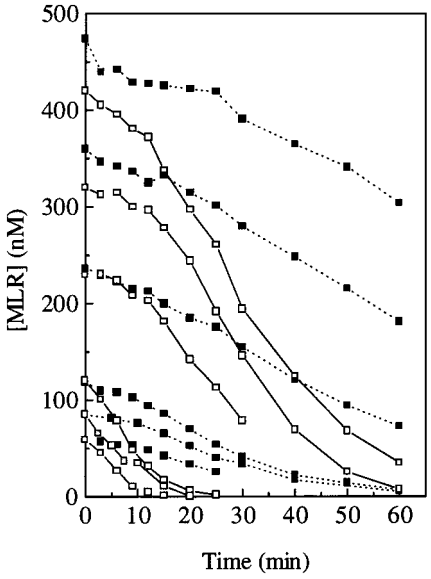

FIGURE 6. Microcystin-LR removal from suspension at pH 3.5 and 8.6. Solid lines through open squares correspond to pH 3.5 data and dotted lines through solid squares to pH 8.5 data.

but at high concentrations of MLR a distinct lag before degradation is observed. A similar lag is also apparent in all photodegradation experiments at pH 8.5. As noted earlier, the higher pH degradation rates are significantly lower than at pH 3.5 but demonstrate a similar decrease on increase in toxin concentration as found in the lower pH case (Figure 6). As will be discussed in some detail below, these effects are presumably related to competitive phenomena involving

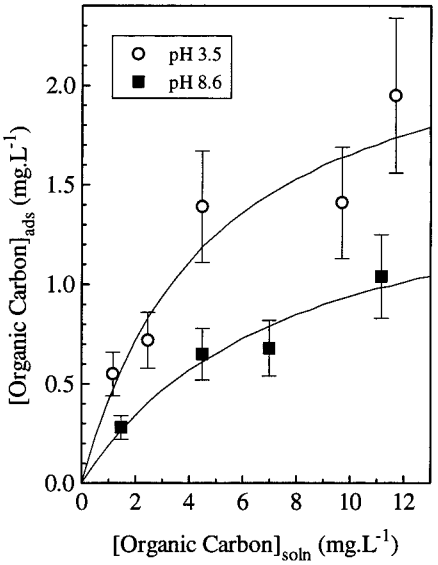

FIGURE 7. Adsorption isotherms for uptake of organic carbon (principally cyanobacterial exudate) onto 1 g·L^{-1} TiO_2 from solutions of pH 3.5 and 8.6.

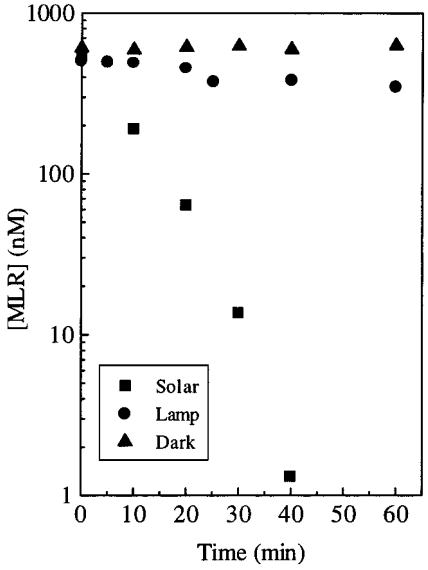

FIGURE 8. Comparison of extent of removal of microcystin-LR from pH 6.4 solutions as a function of time in the dark, in the presence of 365 nm light and on photolysis with midday solar radiation. Initial toxin concentration of 500 nM and 1 g·L^{-1} TiO_2 used in each case.

the large amount of nonspecific cyanobacterial exudate present compared to the trace concentrations of toxin. As shown in Figure 7, this organic matter adsorbs significantly to the TiO_2 suspension both at low and high pH. Rectangular hyperbolae may be fitted to this sorption data yielding conditional adsorption constants of $10^{2.3}$ and $10^{2.1}$ L/g and maximum adsorption capacities of 2.1 and 1.7 mg/L at pH 3.5 and 8.6, respectively.

While microcystin toxins have been reported to be stable at elevated temperatures (*35*), the rate of photocatalytic degradation of MLR in the heterogeneous mixture increases with increase in temperature. An Arrhenius plot (figure not shown) of the temperature-dependent rates yields an activation energy (E_a) on the order of 59 kJ/gmol. Such a value is indicative of a surface-controlled rather than a transport-controlled process for which, typically, E_a < 20 kJ/gmol (*35*).

As can be seen from Figure 8, a large variation in reaction rates is observed between a sample less intensely irradiated using natural (solar) light compared to a sample irradiated

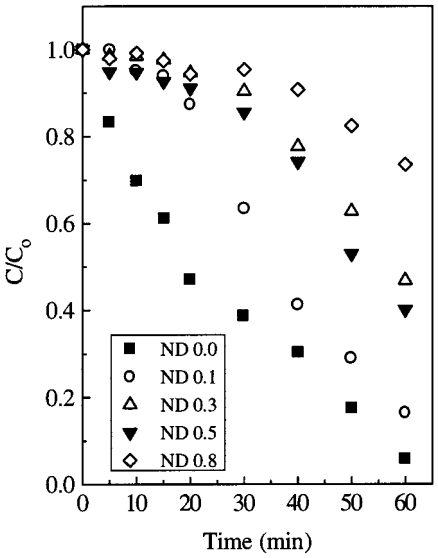

FIGURE 9. Comparison of extent of removal of microcystin-LR from 365 nm photolyzed solutions in the presence of 1 g·L^{-1} TiO_2 at various light intensities as set by the use of neutral density filters. Initial toxin concentration of 85 nM used in each case.

using the near-UV lamp. While the total irradiation provided by the near-UV lamp is at least 10 times that of the solar spectrum (55 mW/cm^2 compared to 4.4 mW/cm^2), the initial rate of degradation of MLR at pH of 6.4 on exposure to solar light is 1.1×10^{-9} M/s compared to 5.4×10^{-11} M/s on exposure to near-UV light. Exponential decay of MLR is observed in both near-UV and solar photolyzed cases with pseudo-first-order decay rates of 0.0065 and 0.135 min^{-1}, respectively.

Figure 9 confirms that the removal rate for the UV lamp system are light intensity dependent with the rate decreasing with decreasing light intensity though after an initial lag at this pH (6.4). The delay before significant toxin removal from solution occurs appears to lengthen with decreasing light intensity.

Discussion

The results reported above (and particularly those shown in Figure 2) suggest that a TiO_2-catalyzed photodegradation process is responsible, in general terms, for the observed reduction in microcystin-LR concentration in the presence of near-UV and solar radiation. The temperature dependence of the degradation process supports the hypothesis that the reaction is surface-controlled. The observed effect of pH on initial degradation rate, and the close correlation to the pH dependence of MLR adsorption to TiO_2, suggests that an adsorbed species plays a central role in the removal of MLR from solution. Apparent anomalies however are present. For example, if the presence of an adsorbed species is critical to effective toxin degradation, why does MLR degradation occur at high pH, albeit after a brief lag, where toxin adsorption is negligible? What process determines the occurrence and extent of the observed lag at pHs in the neutral to basic regions? While MLR removal appears to follow pseudo-first-order kinetics in the acidic pH region, the effect of increase in initial MLR concentration might suggest otherwise. These issues are examined in further detail below.

As mentioned above, the adsorption of microcystin-LR to TiO_2 appears to be an important step in the light-enhanced removal of toxin from acidic suspensions. As shown in Figure 4, experimental evidence suggests a very strong pH dependence of MLR uptake to TiO_2. That this is to be expected for this toxin is easily seen from simple surface complexation modeling of the adsorption process.

TABLE 1. Reactions and Associated Constants Used in Surface Complexation Model of Microcystin-LR Interaction with TiO_2 Surface Hydroxy Groups

no.	reaction	log *K*	ref
1	$>TiOH_2^+ = >TiOH + H^+$	2.6	36
2	$>TiOH = >TiO^- + H^+$	9.0	36
3	$MLRH_3^+ = MLRH_2^0 + H^+$	3.0	43, 44
4	$MLRH_2^0 = MLRH^- + H^+$	3.0	43, 44
5	$MLRH^- = MLR^{2-} + H^+$	12.5	42
6	$>TiOH + MLRH^- + H^+ = >TiMLRH + H_2O$	8.0	this paper
7	$>TiOH + CO_3^{2-} + H^+ = >TiCO_3^- + H_2O$	13.0	45

The chemical reactions and the associated constants required to develop a single site-type, diffuse double layer single surface complex model of microcystin-LR adsorption to TiO_2 are shown in Table 1. First and second acidity constants for TiO_2 range significantly, and we have adopted values ($pK_{a1} = 2.6$ and $pK_{a2} = 9.0$) previously been determined by Yates and Healy (*36*) based on preliminary titration experiments. A surface area of 10 m^2/g as reported by the manufacturer (*37*) and a site density for surface hydroxyl groups of 2.4 sites/nm^2 (equivalent to approximately 4×10^{-6} mol/m^2 or 4×10^{-5} mol/L for this oxide) in accord with the results of Boehm and co-workers from studies on Degussa P-25 TiO_2 (*38*) have been used in all calculations. The value of 2.4 OH sites/nm^2 used here is close to the value of 1.79 sites/nm^2 determined by Rodriguez et al. (*39*) from hydroxyl ion adsorption studies and 1.7 sites/nm^2 from fluoride exchange capacity studies by van Veen et al. (*40*) (in both cases for the Degussa P-25 substrate rather than the Tioxide TiO_2 used in this study) but lower than the value of 3.8 sites/nm^2 determined by Vasudevan and Stone (*41*).

Microcystin-LR has three main functional groups which impart the molecule's acid−base functionality—two acid groups (erythro-*b*-methyl aspartic acid and D-glutamic acid) and a basic group (L-arginine). The two amino acid groups possess unusual peptide bonds between the side chain COOH group and the amine group, leaving the α-COOH group free. The resulting bond exhibits some electron withdrawing influence on the α-COOH group raising the pK_a's from 2.0 and 2.2 for erythro-*b*-methyl aspartic acid and D-glutamic acid (*44*), respectively, to approximately 3.0 for both groups (*43*, *44*).

While no information is available on the precise nature of the surface complex formed with microcystin-LR, we have assumed that the reaction has a stoichiometry resulting in formation of a neutral complex, >TiMLRH (reaction 6, Table 1). In addition, while insignificant in the acidic pH range, carbonate anions have also been reported to adsorb to >TiOH surface groups (*45*) and a reaction to this effect has been included in the sorption model (reaction 7, Table 1). Using the optimization code FITEQL (*46*) and the geometric estimate for the number of sites, a formation constant of $10^{8.0}$ is obtained for the microcystin-LR surface complex. As can be seen from Figure 4, the resulting surface complexation model closely describes the dark adsorption data with a sharp peak in adsorption at a pH of approximately 3.5. Electrostatic replusion between the protonated toxin molecules and positively charged surface sites limits uptake at lower pH, while repulsive effects between deprotonated surface sites and toxin acid groupings limit uptake at pHs in the basic region ($pH_{pzc} \cong 6.4$ for TiO_2).

It is worth noting that, in the studies undertaken here, there is superficially a large excess of reactive TiO_2 hydroxy surface sites ($[TiOH]_{TOT} \cong 4.0 \times 10^{-5}$ moles/L) compared to sorbing substrates. At pH of 3.5, where maximum toxin uptake is observed, no more than approximately 0.3% of sites are apparently occupied by microcystin-LR (as shown

previously, $[MLR]_{ads}^{max}$ 1.3×10^{-7} mol/L at pH 3.5). The total concentration of other cyanobacterial exudates is high compared to the microcystin-LR concentration present but, even assuming a relatively low mean molecular weight of 1000 for this ill-defined organic matter, supposedly no more than 5.3% of total available sites are occupied by this material (recall that $[cyanobacterialexudate]_{ads}^{max} = 2.1$ mg/L or 2.1×10^{-6} mol/L for an assumed molecular weight of the cyanobacterial exudate of 1000).

The large number of reactive TiO_2 hydroxy surface sites however is somewhat misleading since the MLR and particularly cyanobacterial exudate (denoted below as CE) molecules are large (e.g. proteins) and when adsorbed are likely to deactivate (block) portions of the TiO_2 surface. Assuming that there are 2.4 sites/nm^2 on the TiO_2 particle and using a space filling model to estimate the size of the MLR molecule (approximately 1.2 nm × 1.8 nm side on and 1.8 nm × 1.4 nm face down), MLR would cover approximately 5−6 sites with only one of these a binding site. If the average molecular weight of cyanobacterial exudate is 1000−10 000, such large CE molecules are potentially blocking about 5−50 sites, seriously limiting MLR attachment. This may partly explain why the maximum adsorption of MLR (1.3×10^{-7} mol/g) is much (300 times) lower than the number of geometrically estimated surface sites (4×10^{-5} mol/g). A significant (though less dramatic) difference is also apparent from Robertson et al.'s work (*31*) where a maximum of 2.5 $\times 10^{-5}$ mol of purified MLR is estimated to be adsorbable per gram of TiO_2, whereas the geometrically estimated surface site concentration is 1.7×10^{-4} mol of sites/g of TiO_2. The fact that the maximum MLR adsorption attainable (as a proportion of total available sites) in our studies is significantly less than that found by Robertson et al. (*31*) is presumably the result of the presence of cyanobacterial exudate (which competes for surface sites). Indeed, when allowance is made for the adsorbing capacity of the exudate in FITEQL modeling, we obtain a conditional log *K* value for MLR adsorption very close to the $10^{4.1}$ M^{-1} found by Robertson et al. (*31*).

Initial removal rate of toxin at 85 nm MLR closely follows MLR adsorption in the acidic pH. A portion of this removal could be attributed to sorptive uptake to the TiO_2 surface, but, under illuminated conditions, the extent of toxin removal is far greater than can be accounted for by adsorption alone. For example, at pH 3.5, a maximum dark removal of approximately 40 nM MLR is observed, while, in the light, complete (exponential) removal of 85 nM MLR occurs within about 20 min of photolysis. At pH ≈ 6, no more than a few percent of toxin is adsorbed in the dark, but, on photolysis, complete removal is observed within 30−40 min. Hence, while adsorption kinetics could be responsible for the rate of removal of MLR from the suspension, the uniform first-order nature of removal over the full extent of removal suggests that the rate controlling step is, rather, surface mediated catalyzed breakdown of MLR.

While not always justified (*47*), it has been common under conditions where adsorption is the (rapid) precursor to a rate controlling surface-mediated degradative step, to assume that the initial rate of contaminant removal is dependent upon both an equilibrium adsorbed contaminant concentration and the concentration of surface-located oxidizing species (*48*, *49*). Under these conditions, an expression for the initial rate of removal of microcystin-LR may be written as

$$\frac{-\mathrm{d}[MLR]}{\mathrm{d}t} = k \cdot [>TiMLRH] \cdot [\text{oxidizing species}] \quad (3)$$

If the concentration of the oxidizing species rapidly attains some steady-state concentration, this expression may be simplified to the pseudo-first-order form

$$\frac{-\mathrm{d}[MLR]}{\mathrm{d}t} = k' \cdot [>TiMLRH] \quad (4)$$

in which case prediction of the extent of toxin adsorption may be used to predict the initial rate of toxin removal.

In reality of course, contaminant adsorption is unlikely to be instantaneous, and assumption that sorptive equilibrium is reached is likely to be flawed. The extent of departure of the actual kinetic behavior from that predicted by eq 4 will be dependent, at least in part, upon the relative rates of adsorption and degradation.

Elucidation of the effects of increasing MLR concentration may be complicated by the fact that as toxin concentration is increased, so too is that of the accompanying (and potentially site limiting) ill-defined cyanobacterial exudate (denoted below as CE). The situation with respect to photoassisted toxin removal rates is further complicated by a decrease in reaction rates on increasing MLR (and CE) concentrations at both low (3.5) and high (8.6) pH (Figure 6). If the geometric estimate for the surface site density is replaced with the Langmuir derived maximum adsorption of MLR at pH 3.5 ($\log K_{ads} = 10.8$), some of the rather unusual photodegradation behavior at low and high pH may be explained. At low pH and low MLR concentrations, where adsorption of neither MLR nor CE is limited by site availability, direct competition for surface-located oxidizing species between MLR and CE could account for MLR's apparent pseudo-first-order degradation behavior. As MLR and CE concentrations are increased to limiting adsorption values the proportion of total MLR and CE adsorbed decreases, and there is a subsequent initial lag followed by rapid MLR degradation.

The possibility exists that most of the surface-generated hydroxyl radicals generated in the primary photophysical process are scavenged by the ill-defined CE that is present in large excess of MLR with subsequent degradation of the toxin by CE free radicals. These CE radicals may also presumably react with other CE components and, as a result, lose their oxidizing ability. Thus, whether the effective oxidizing species are organic radicals (arising from oxidation of CE) or hydroxyl radicals directly, an increase in CE concentration (as MLR concentration is increased) might be expected (qualitatively at least) to produce the behavior shown in Figure 6.

We are obliged to be a little more speculative with regard to likely processes operating at high pH where the toxin degradation rates are initially low but, after a lag, become substantial. Such effects may be realized by the release of long-lived oxidizing species (most likely organic peroxy radicals derived from oxidation of CE or carbonate radicals) to solution which, in turn, oxidize the dissolved MLR. Initial concentrations of CE free radicals in solution will be low with the result that the bimolecular degradation of toxin molecules will be slow. An increase in degradation rate would be expected as the concentration of exudate radicals in solution increases (i.e. after a lag period). Such a process will not be important at low pH and low toxin concentration where adsorption is not limiting at the TiO_2 surface. At high pH, the proposed mechanism becomes important because of the adsorption (with subsequent oxidation and release to solution) of CE but not MLR.

While it is proposed that long-lived CE radicals are produced as a result of interaction with the product of the primary photoprocess (holes or hydroxyl radicals), the precise mechanism by which this occurs is unclear. The process however may be considered to be a form of spin trapping to produce long-lived adducts. These adducts may be similar to the long-lived intermediates produced on photolysis of natural organic matter which have been reported to be effective oxidants of a variety of phenolic compounds (*50*).

The marked increase in rate of removal of MLR when changing from 365 nm irradiation to irradiation with a full solar spectrum is noteworthy (Figure 8). While quantum efficiency for wide band gap semiconductors has been shown to decrease as a function of one over the square root of the absorbed light intensity (*51*), the 20-fold increase in reaction rate at the lower solar irradiation was unexpected. This cannot be accounted by an increase of temperature for the solar conditions or by reaction with dissolved organic matter (DOM) derived photoreactants (Figure 2) (*52*). It is therefore suggested that components of the CE (possibly natural dye components such as chlorophyll a, β-carotene, zeaxanthrin, or echinenone (*53*)) enhance oxidation via visible photosensitization with TiO_2. Injection of electrons from adsorbed excited dye molecules into the conduction band of the TiO_2 particle when exposed to the full solar spectrum have the capacity to form cation dye radicals (*54*, *55*). Such photogenerated dye radicals either undergo further self-degradation or may presumably react with adsorbed or solution MLR. Further work isolating natural dye components and forming organotitanium dioxide complexes for visible photosensitization will quantify this potential important reaction pathway.

Acknowledgments

Support provided to A.F. through DEET in the form of an APA-I scholarship is gratefully acknowledged as is the support provided by the industry partner, Hunter Water Australia. Cheryl Orr is thanked for provision of assistance with some of the MLR analyses as is Arne Ressl for conducting some of the experiments. Stefan Hug (EAWAG) is acknowledged for his helpful suggestions on possible mechanisms of contaminant removal.

Literature Cited

(1) Jones, G. J. In *Waterplants in Australia*: Sainty, G. R., Jacobs, S. W. L., Eds.; Sainty and Associates: Darlinghurst, NSW, 1994.
(2) Lawton, L. A.; Codd, G. A. *J. Inst. Water Environ. Management* **1991**, *5*, 460.
(3) State Algal Coordinating Committee. *Implementing the New South Wales Algal Management Strategy, Annual Report 1993−1994*; Department of Water Resources: Parramatta, Sydney, 1994.
(4) Falconer, I. R.; Beresford, A. M.; Runnegar, T. C. *Med. J. Austral.* **1983**, *1*, 511.
(5) Carmichael, W. W. *Sci. Am.* **1994**, *270*, 64.
(6) Stoner, R. D.; Adams, W. H.; Slatkin, D. N.; Siegelman, H. W. *Toxicon.* **1989**, *27*, 825.
(7) Carmichael, W. W.; Mahmood, N. A.; Hyde, E. G. In *Marine Toxins: Origin, Structure, and Molecular Pharmacology*; Hall, S., Strichartz, G, Eds.; American Chemical Society: Washington, DC, 1990; p 87.
(8) Nishiwaki-Matsushima, R.; Ohta, T.; Nishiwaki, S.; Suganama, M.; Kohyama, K.; Ishikawa, T.; Carmichael, W. W.; Fuuki, H. *J. Cancer Res. Clin. Oncol.* **1992**, *118*, 420.
(9) McKnight, D. M.; Chisholm, S. W.; Harleman, D. R. F. *Environ. Manag.* **1983**, *7*, 311.
(10) Jones, G. J.; Orr, P. T. *Water Res.* **1994**, *28*, 871.
(11) Hoffmann, J. R. H. *Water S. A.* **1976**, *2*, 58.
(12) Velzeboer, R.; Drikas, M.; Donati, C.; Burch, M.; Steffensen, D. *Proceedings AWWA 16th Federal Convention, 1995, Sydney*; Australian Water and Wastewater Association Inc.: Artarmon, Sydney, 1995; Vol. 1, pp 121−128.
(13) Nicholson, B. C.; Rositano, J.; Durch, M. D. *Water Res.* **1994**, *28*, 1297.
(14) Jones, G. J.; Minato, W.; Craig, K.; Naylor, R. Proceedings AWWA 15th Federal Convention, 1993, Gold Coast; Panther Publishing: Canberra, 1993; Vol. 2, pp 339−346.
(15) Craig, K.; Bailey, D. *Proceedings of the AWWA 16th Federal Convention, 1995 Sydney*; Australian Water and Wastewater Association Inc.: Artarmon, Sydney, 1995; Vol. 2, pp 579−586.
(16) Jones, G. J.; Falconer, I. F.; Wilkins, R. M. *Environ. Toxicol. Wat. Qual.* **1995**, *10*, 19.
(17) Jones, G. J.; Bourne, D. G.; Blakeley, R. L.; Doelle, H. *Natural Toxins* **1994**, *2*, 228.
(18) Fawell, J. K.; Hart, J.; James, H. A.; Parr, W. *Water Supply* **1993**, *11*, 109.
(19) Harada, K.-I.; Ogawa, K.; Matasuura, K.; Murata, H.; Suzuki, M.; Watanabe, M. F.; Itezono, Y.; Nakayama, N. *Chem. Res. Toxicol.* **1990**, *3*, 473.
(20) Harada, K.-I.; Matsauura, K.; Suzuki, M.; Watanabe, M. F.; Oishi, S.; Dahlem, A. M.; Beasley, V. R.; Carmichael, W. W. *Toxicon.* **1990**, *28*, 55.
(21) Ollis, D.F.; Pelizzetti, E.; Serpone, N. *Environ. Sci. Technol.* **1991**, *25*, 1523.
(22) Jaeger, C. D.; Bard, A. J. *J. Phys. Chem.* **1979**, *84*, 3146.
(23) Matthews, R. W. *J. Chem. Soc., Faraday Trans.* **1984**, *80*, 457.
(24) Okamoto, K.; Yammoto, Y.; Tanaka, H.; Tanaka, M.; Itaya, A. *Bull. Chem. Soc. Jpn.* **1985**, *58*, 2015.
(25) Martin, S. T.; Lee, A. T.; Hoffmann, M. R. *Environ. Sci. Technol.* **1995**, *29*, 2567.
(26) Minero, C.; Pelizzetti, E.; Malato, S.; Blanco, J. *Chemosphere* **1993**, *26*, 2103.
(27) Serpone, N.; Borgarello, E.; Harris, R.; Cahill, P.; Borgarello, M.; Pelizzetti, E. *Solar Energy Materials* **1986**, *14*, 121.
(28) Palmsiano, L.; Augugliaro, V.; Schiavello, M.; Sclafani, A. *J. Mol. Catal.* **1989**, *56*, 284.
(29) Alberici, R. M.; Jardim, W. *Water Res.* **1994**, *28*, 1845.
(30) Suri, R. P. S.; Lui, J.; Hand, D. W.; Crittenden, J. C.; Perram, D. L.; Mullins, M. E. *Water Environ. Res.* **1993**, *65*, 665.
(31) Robertson, P. K. J.; Lawton, L. A.; Munch, B.; Rouzade, J. *Chem. Commun.* **1997**, *4*, 393.
(32) Szymczak, R.; Waite, T. D. *Aust. J. Mar. Freshwater Res.* **1988**, *39*, 289.
(33) Tsuji, K.; Nalto, S.; Kondo, F.; Ishikawa, N.; Watanabe, M. F.; Suzuki, M.; Harada, K.-H. *Environ. Sci. Technol.* **1994**, *28*, 173.
(34) Matthews, R. W.; McEvoy, S. R. *Solar Energy* **1992**, *49*, 507.
(35) Locker, L. D.; de Bruyn, P. L. *J. Electrochem. Soc.* **1969**, *116*, 1659.
(36) Yates, D. E.; Healy, T. W. *J. Chem. Soc., Faraday Trans. I* **1980**, *76*, 9.
(37) Tioxide Group, Tioxide A-HR Technical Information, 1984.
(38) Herrmann, V. M.; Boehm, H. P. *Z. Anorg. Allg. Chem.* **1969**, *368*, 73.
(39) Rodriguez, R.; Blesa, M. A.; Regazzoni, A. E. *J. Colloid Interface Sci.* **1996**, *177*, 122.
(40) van Veen, J. A.; Veltmaat, F. T. G.; Jonkers, G. *J. Chem. Soc., Chem. Commun.* **1985**, 1656.
(41) Vasudevan, D.; Stone, A. T. *Environ. Sci. Technol.* **1996**, *30*, 1604.
(42) *Practical Handbook of Biochemistry and Molecular Biology*; Fasman, G. D. Ed.; Lewis Publishers: Boca Raton, FL, 1989.
(43) *Principles and Techniques of Practical Biochemistry*; Wilson, K., Walker, J. M. Eds.; Cambridge University Press: Cambridge, 1994; p 166.
(44) Rivasseau, C.; Martins, S.; Hennion, M.-C. *J. Chromatography A* **1998**, *799*, 155.
(45) Kormann, C.; Bahnemann, D. W.; Hoffmann, M. R. *Environ. Sci. Technol.* **1991**, *25*, 494.
(46) Hebelin, A.; Westall, J. C. FITEQL 3.1. Report 94-01, Department of Chemistry, Oregon State University, 1994.
(47) Cunningham, J.; Al-Sayyed, G.; Srijaranai, S. In *Aquatic and Surface Photochemistry*; Helz, G. R., Zepp, R. G., Crosby, D. G., Eds.; Lewis Publishers: Boca Raton, FL, 1994; p 317.
(48) Hoffman, M. R.; Martin, S. T.; Choi, W.; Bahnemann, D. W. *Chem. Rev.* **1995**, *95*, 69.
(49) Ollis, D. F.; Pelizzetti, E.; Serpone, N. In *Photocatalysis: Fundamentals and Applications*; Serpone, N., Pelizzetti, E., Eds.; John Wiley & Sons: New York, 1989; pp 603−637.
(50) Canonica, S.; Hoigne, J. *Chemosphere* **1995**, *30*, 2365.
(51) Bahnemann, D.; Cunningham, J.; Fox, M. A.; Pelizzetti, E.; Pichat, P.; Serpone, N. In *Aquatic and Surface Photochemistry*; Helz, G. R., Zepp, R. G., Crosby, D. G., Eds.; Lewis Publishers: Boca Raton, FL, 1994; p 216.
(52) Hoigné, J. In *Aquatic Chemical Kinetics*; Stumm, W., Ed.; John Wiley & Sons: New York, 1990; p 43.
(53) Walsh, K.; Jones, G. J.; Dunstan, H. J. *Phytochemistry* **1997**, *41*, 817.
(54) Hodak, J.; Quinteros, C.; Litter, M. I.; san Román, E. *J. Chem. Soc., Faraday Trans.* **1996**, *92*, 5081.
(55) Vinodgopal, K.; Wynkoop, D. E.; Kamat, P. *Environ. Sci. Technol.* **1996**, *30*, 1660.

Received for review October 30, 1997. Revised manuscript received July 23, 1998. Accepted October 8, 1998.

ES970952D